INVESTIGATION OF NORMAL IONIZING SHOCK WAVES IN ARGON

Raymond Joseph Hogan

NAVAL POSTGRADUATE SCHOOL
Monterey, California

THESIS

INVESTIGATION OF NORMAL IONIZING
SHOCK WAVES IN ARGON

by

Raymond Joseph Hogan

Thesis Advisor: A.W. Cooper

June 1972

Investigation of Normal Ionizing Shock Waves in Argon

by

Raymond Joseph Hogan
Ensign, United States Navy
B.S., United States Naval Academy, 1971

Submitted in partial fulfillment of the
requirements for the degree of

MASTER OF SCIENCE IN PHYSICS

from the

NAVAL POSTGRADUATE SCHOOL
June 1972

ABSTRACT

Normal ionizing shock waves in neutral argon gas were generated using a cylindrical theta pinch. Axial propagation of these shock waves has been investigated using photoelectric detectors. Magnetic and electrostatic probes were used to give additional information regarding shock structure. The investigation was carried out using steady state magnetic fields normal to the shock front, with a maximum field of 7200 gauss. Initial gas pressures ranged from 0.02 to 1.0 Torr. The investigations included studies of the effects of initial pressure, magnetic field, and capacitor bank voltage upon the shock velocity. Included is a brief discussion of the theta pinch along with the current theory of normal ionizing shock waves.

TABLE OF CONTENTS

ACKNOWLEDGEMENT

Several people have given much help during this investigation. To Professor A.W. Cooper who has acted as advisor and contributed many new ideas, to Hal Herreman who always had a solution to the daily problems encountered, and to Mike O'Shea my coworker, I extend many thanks.

Thanks are also extended to the Naval Ordnance Laboratory, White Oak, and the Office of Naval Research which jointly sponsored this project, under Project order number P.O. 0-0153, and provided the necessary funding.

I. INTRODUCTION

This study is a single portion of a continuing project calling for investigation of shock wave generation and propagation. This segment of the investigation involves the study of normal ionizing shock waves. An ionizing shock wave is defined as a wave which propagates into a neutral, nonconducting gas, causing ionization and results in a finite conductivity plasma in the postshock state.

Ionizing shock waves are of interest as a method of production of high temperature, high pressure thermalized plasmas, because of the applicability to certain astrophysical events, and for plasma propulsion devices. Normal ionizing shock waves bear a very definite kinship to classical detonation waves. This similarity results from the analogy between the Joule heating, which takes place in the ionizing fronts and the chemical heating within the fronts of detonation waves.

This report concerns the investigation of normal ionizing shock waves (the preshock magnetic field is normal to the shock front) generated by the discharge of a 13.1 kJ fast capacitor bank through a single turn theta pinch coil. Modifications of the existing system including the incorporation of a time-resolved spectrographic unit are discussed along with photomultiplier and probe studies of the propagating luminous front. A brief history of major experimental investigations as well as a summary of recent theoretical descriptions of normal ionizing shock waves is included.

II. BACKGROUND

A. HISTORY

1. Shock Wave Studies at The Naval Postgraduate School Plasma Facility Theta Pinch

Design and construction of the present single turn theta pinch system was begun by Budzik [1] and completed through preliminary testing by Christensen [2]. This system was modified for spectroscopic investigation of ionizing fronts in this most recent study.

Prior to the construction of the present system, two previous attempts to produce shock waves had been made at the plasma facility. A multiturn coil surrounding the plasma column and driven by an RF transmitter was used by Andrews [3]. The transmitter operated in the 100 to 500 kHz range and had a maximum power output of 2kW. This system resulted in an energy input of 8×10^{-3} joules per cycle at a frequency of 250 kHz. This attempt to produce shock waves along a nitrogen plasma column was interrupted by the appearance of unexplained fluctuations in the plasma column.

The second shock wave generation study was performed by Beam [4]. This investigation utilized a 0.75 μF capacitor bank with a rated voltage of 20 kV which discharged through a single turn theta pinch type coil. The results of this system were found to be not reproducible.

2. Experimental Investigations of Normal Ionizing Shock Waves

The majority of the experimental investigations of normal ionizing shock waves have utilized the electromagnetic shock tube for wave generation. The development of that device in the 1950's marked the initiation of significant investigations in this area. Almost all of the important measurements made have been in cylindrical electromagnetic tubes of the coaxial type.

Normal ionizing shock waves were produced in early experiments, but these attempts lacked reproducibility and gave inconsistent results [5]. The first investigation yielding extensive quantitative results with nearly constant wave speeds was conducted by Heywood [6], using a coaxial electromagnetic shock tube. Velocity measurements indicated that the shock speed could be accurately represented by a simple snow-plow type model. Electric field measurements in the preshock gas by Heywood were the first to give qualitative verification of the theory of Taussig [7]. This theory will be discussed in the following chapter. Measurements were made in the trans-Alfvénic region (shock speeds between one and three times the Alfvén speed in the preshock gas) and in the super-Alfvénic region (shock speeds greater than three times the Alfvén speed). Heywood was unable to find evidence of hydrodynamic switch-on behavior (the appearance of a transverse component of magnetic field) in the trans-Alfvénic region or gasdynamic behavior in the super-Alfvénic region as predicted by Taussig's theory.

The first direct verification of switch-on shocks in the trans-Alfvénic regime was made by Miller [8]. Magnetic field

measurements indicated that there was no separation between the shock itself and the drive currents. The absence of a current-free post-shock state was in keeping with the theory of Kunkel and Gross [9], which predicted Chapman-Jouguet behavior. The Chapman-Jouguet hypothesis predicts that the face of the rarefaction wave travels at the same speed as the shock. This implies that there will be no region of uniform plasma between the two waves.

The most extensive and most recent experiments in this area are those carried out by Levine [5]. Here, shock speeds were measured as a function of initial gas pressure drive current, and applied axial magnetic field. Again, a coaxial electromagnetic shock tube was employed. His investigation showed that trans-Alfvénic shocks exhibit Chapman-Jouguet behavior. Normal ionizing shock waves in the super-Alfvénic regime were found to be gas dynamic in nature.

To date, no detailed study of sub-Alfvénic normal ionizing shock waves has been carried out. All the major efforts in this area have dealt with trans-Alfvénic and super-Alfvénic shocks and have produced these in electromagnetic shock tubes.

Miller [8] has performed limited investigations in the sub-Alfvénic region. The major result of this investigation was the verification of switch-on behavior of the shocks.

B. THE THETA PINCH EQUIPMENT

The theta pinch capacitor bank consists of six 7 μF capacitors. The capacitors are connected in parallel by 8.8 cm wide copper strip lines to the theta pinch coil. Each capacitor is connected in series with a pressurized four-element spark gap. Breakdown

of the spark gap allows discharge of the capacitor through the pinch coil to ground. These six spark gaps are fired simultaneously by a master spark gap charged to 30 kV. The signal from the master gap is transmitted to the slave gaps by six coaxial cables. The master gap is fired by 48 volt thyratron pulse. A complete description of the theta pinch equipment can be found in Budzik [1]. The most important parameters of the theta pinch assembly are summarized below.

Maximum charging voltage	25 kV
Capacitance	42 μF
Maximum stored energy	13.1 kJ
Peak current	255 kA
Peak flux density	20 kG
Discharge ringing frequency	156 kHz
Initial current rise time	1.6 μs
Coil length	14.5 cm
Coil diameter	5.5 cm

C. THE STREAK CAMERA AND DISPERSION UNIT

A Beckman and Whitley time resolving equipment group was used for spectroscopic investigation of the radiation produced by the passage of the theta pinch-produced ionizing shock wave. The equipment group consists of the model D-2 spectroscopic dispersion unit and the model 339 continuous writing streak camera.

The streak camera is specifically designed for the study of events whose time of occurrence within the camera field of view cannot be accurately predicted. It is therefore well suited for recording events such as the passage of a luminous shock front.

The film remains stationary and is swept by a traveling image reflected by a turbine driven beryllium mirror. The mirror speed is controllable up to a maximum rotational speed of 2600 revolutions per second. This maximum speed corresponds to a writing rate of 9 mm per microsecond, and a minimum writing time of 131 microseconds. Attachment of the dispersion unit allows a time resolved spectral record of the event to be displayed on film. Further specifications of the spectroscopic dispersion unit can be found in Appendix A.

III. THEORY

A. THE THETA PINCH

The production of radially directed shock waves in a pre-existing plasma by a theta pinch device has been well researched both experimentally and theoretically. The passage of a current pulse through the pinch coil produces a rapidly rising induction field within the dimensions of the coil. The highly conducting plasma within the pinch coil region reacts to this increasing axial induction field by the formation of a current sheath, the current in the sheath being azimuthal and in the opposite direction to that of the coil. This sheath acts to prevent diffusion of the field into the plasma-filled coil region. A representation of this induced current sheath within the plasma is shown in Figure 1 below, where J_c is the coil current and J_p the plasma sheath current.

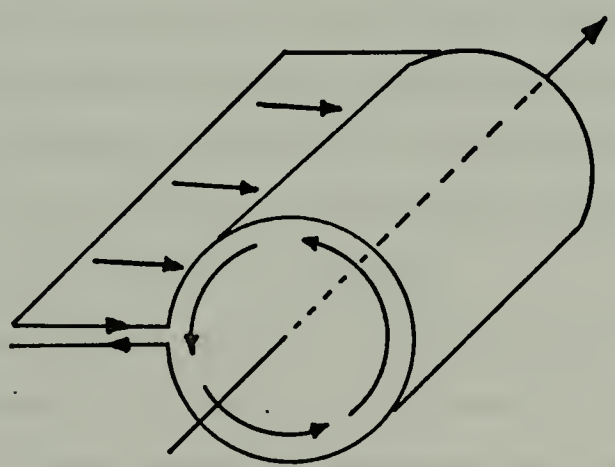

Figure 1. The Theta Pinch Coil and the Plasma Current Sheath

In the limit of a plasma having infinite conductivity, this sheath current will be equal in magnitude but oppositely directed to the current in the coil. The motion of the particles within the current sheath will cause an interaction with the magnetic field resulting in a $\bar{J} \times \bar{B}$ force which can be considered as acting upon the entire sheath. This force is directed radially inward and causes the current sheath to collapse radially inward. As the sheath propagates toward the coil center, it sweeps up essentially all of the charged particles contained within the dimensions of the coil. This concept is referred to as the snow-plow model of the theta pinch.

In the case of a large current pulse of short duration, the very rapid rise of the magnetic induction field and the increased magnitude of the resulting force produces a radially directed shock wave. A simple but relatively complete model of the theta pinch collapsing shock has been proposed and numerically solved by Hain and Kolb [10]. The theory is based on the two fluid plasma model and though it is one of the simpler approaches it must be numerically solved and involves much mathematical manipulation. For this reason the author has chosen to discuss the initial assumptions and the basic physical relationships which are involved in the solution of the theta pinch problem.

A fully ionized plasma existing within the pinch coil prior to discharge is assumed. The pinch coil is assumed to have cylindrical symmetry and end losses are therefore not considered. The simplifying assumption of quasineutrality gives for the species particle densities $n_e = n_i = n$. This implies from the continuity

equation that

$$v_e = v_i = v.$$

The mass density is given by

$$\rho \approx m_i n$$

because the mass of the electron is negligible.

The form of the continuity equation used in this two fluid model is

$$\frac{d\rho}{dt} + \rho \nabla \cdot \vec{v} = 0$$

where r is the radial distance from the pinch coil center. The momentum equation takes the form

$$\frac{dv}{dt} + \frac{1}{\rho} \frac{\partial}{\partial r} (P_e + P_i + \rho\, q_i) + \frac{1}{\rho} B \frac{\partial B}{\partial r} = 0$$

where $B_z \equiv B$, $v_r \equiv v$, and P_e and P_i are the electron and ion pressures respectively, and q_i is the artificial shockwave term as defined below.

$$q_i = L^2 (\nabla \cdot \vec{v})^2 \qquad \text{for} \quad \nabla \cdot \vec{v} < 0$$

$$q_i = 0 \qquad \text{for} \quad \nabla \cdot \vec{v} \geq 0$$

Here q_i is used to conserve mass, momentum, and energy across the shock front of width L, which is taken to be 1/10 of the radius R.

The initial set of equations is completed by inclusion of the equation giving internal energy ϵ and the equation of state.

$$\epsilon = \frac{P}{\gamma - 1} \; ; \quad P = \rho T$$

These basic equations along with additional relations involving assumptions such as the methods of heat conduction and boundary conditions evolve to a set of partial differential equations.

Solution of these equations involves numerical integration through the shock front. Because the problem requires numerical methods a general solutions is not possible.

Hain and Kolb treated the case where the perturbation field is parallel to the steady state field, the antiparallel case, and the zero steady state field case; all with the same initial conditions. They found that for the reversed field (antiparallel) case there was a sharp hump in the density distribution which moves inward with the shock. In the parallel field case, however, the distribution is considerably flatter. The compression time for the reverse field was approximately half that for the parallel field. The reversed field case gave the highest ion temperature. In the zero field case a wave of hot electrons was found to run ahead of the shock wave. In general Hain and Kolb found that the nature of the trapped steady state field had a great effect upon the behavior of the shock. The results of this computer model agree well with experimental observations.

In the current study, the gas within the pinch coil is unionized. In the case of a neutral gas within the coil, no pinch effect is expected, as the conductivity of the preshock gas is zero and the field will diffuse through, and no current sheath is set up. The equation describing the behavior of a transient magnetic field in a plasma is

$$\frac{\partial \vec{B}}{\partial t} = \nabla \times (\vec{v} \times \vec{B}) + \frac{1}{\sigma \mu_o} \nabla^2 \vec{B}$$

where μ_o is the free space permeability, v is the fluid velocity, and σ is the plasma conductivity. In the case of low conductivity

the second term on the right dominates and the equation becomes a typical diffusion equation. In the case of high conductivity, the diffusion term becomes small, the magnetic field is unable to penetrate the plasma, and the time rate of change of the magnetic field must have associated with it a plasma motion. Such is the case for the theta pinch of a highly conducting plasma.

In the neutral gas, however, the time rate of change of magnetic field will create induced electric fields which, in the case of the theta pinch, will be azimuthally directed. The magnitude of the Electric fields will be dependent upon the value of the first time derivative of the magnetic field. If the electric fields are sufficiently strong, breakdown of the gas will occur resulting in ionization. This ionization will result in increased conductivity. As conductivity increases, the second term of the above equation will no longer dominate and motion of the charged particles will result. In the case of the theta pinch this motion will take the form of the aforementioned current sheath. If breakdown ionization does occur, the pinch effect will necessarily follow. The degree to which the pinch effect dominates the magnetic field diffusion effect is entirely dependent upon the degree of ionization, reflected in the conductivity.

B. IONIZING SHOCK WAVES

When the charged particles are swept to the center of the pinch coil, a high density, high kinetic pressure region is formed. These particles are radially confined by the high magnetic pressure of the induction field surrounding them. In the longitudinal

direction, there is a large pressure gradient formed at the edge of the theta-pinch coil. This pressure discontinuity results in the propagation of a viscous shock wave longitudinally down the column.

This shock wave propagates along the column ionizing the neutral gas as it travels. To be categorized as an ionizing shock, the wave must propagate into a non-conducting un-ionized gas. It must ionize it resulting in a post-shock state which is electrically conducting and therefore subject to electromagnetic interactions. In the case of low velocity shock waves where dissociation but no ionization takes place, the jump conditions can be determined by the standard Rankine-Hugoniot equations for a nonconducting gas. When the shock wave produces ionization, electromagnetic considerations become important, conventional aerodynamic shock wave theory cannot be applied, and a separate ionizing wave theory must be used.

In cases where the magnetic field existing in the preshock gas is perpendicular to the plane of the shock front, the shock is designated a normal shock. If the field is parallel to the shock plane it is a transverse shock. Situations where the field is at some intermediate angle to the shock front plane are known as oblique shocks. At the plasma facility, the steady state field in the preshock gas is longitudinally directed. The shocks being studied are therefore normal shock waves.

Taussig [7] has completed detailed studies of normal ionizing shock waves for ideal gases with and without chemistry. The shock-jump equations without chemistry are listed below.

$$\rho_1 u_1^2 = \rho_2 u_2$$

$$\rho_1 u_2^2 + p_1 = \rho_2 u_2^2 + p_2 + \frac{B_{z2}^2}{8\pi}$$

$$\rho_1 u_1 \left(\frac{u_1^2}{2} + h_1 \right) = \rho_2 u_2 \left[\tfrac{1}{2} \left(u_2^2 + w_2^2 \right) + h_2 \right] + \frac{E_y B_{z2}}{4\pi}$$

$$\rho_1 u_1 w_2 - \frac{B_x B_{z2}}{4\pi} = 0$$

The coordinate system lies in the shock wave rest frame and is elected such that x is perpendicular to the shock surface and y and z are in the plane of the shock. (See Figure 2.) Here u is the normal velocity relative to the shock front and w is the velocity parallel to the front in the z direction. The specific enthalpy for the ideal gas is $h_i = (\gamma/\gamma\text{-}1)p_i/\rho_i$ where i = 1 or 2. E_{L1} is the transverse electric field of the upstream neutral gas. The electric field in the lab system is equal to that in the shock frame because the magnetic field is parallel to the shock velocity and therefore $\vec{u}_1 \times \vec{B}_1 = 0$.

$$\vec{E}_{L1} = \vec{E}_y + \vec{u}_1 \times \vec{B}_1 = \vec{E}_y$$

The initial requirement that the postshock region be steady state requires that there be no current behind the shock so that

$$\vec{E}_2 = - \vec{u}_2 \times \vec{B}_2 .$$

When the conditions of the preshock state are absolutely specified, the post-shock state is uniquely determined by the steady state jump equations and the equations of state for the ideal gas. It is important to note that the electric field ahead of the shock front cannot be arbitrarily specified. This is one of the most

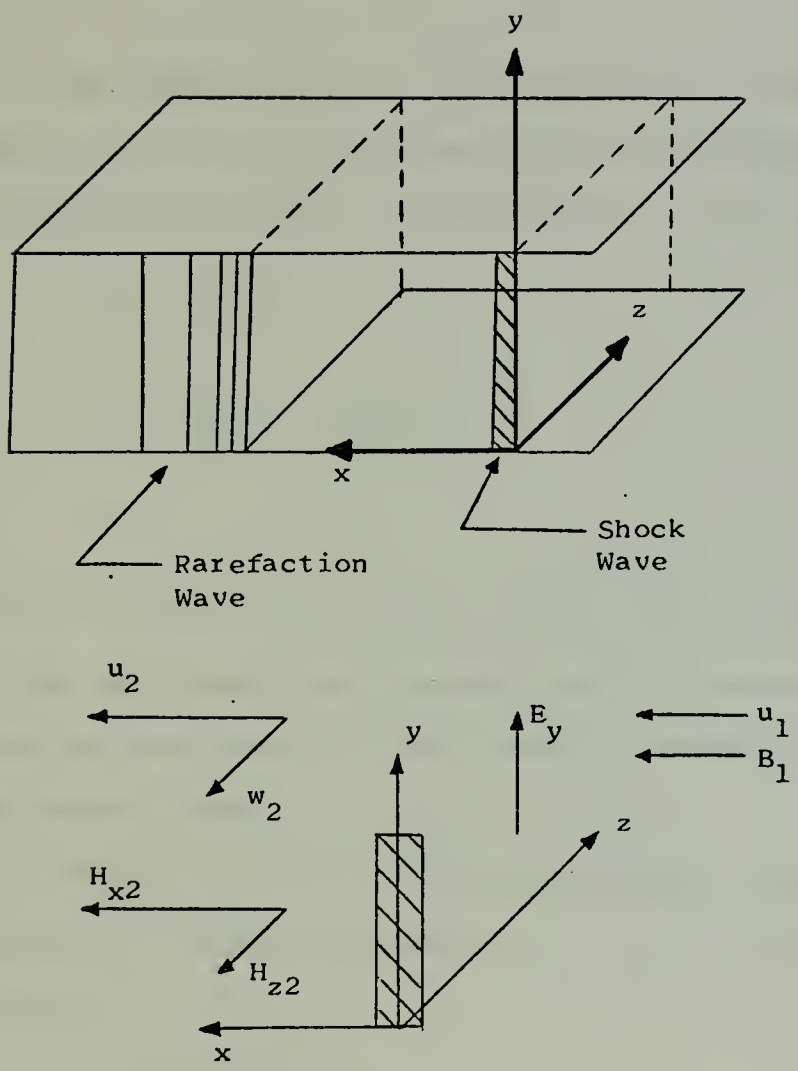

Figure 2. Shock Frame Coordinates

important facts which separates the ionizing shock from the MHD shock where $E_y = 0$ and the gas dynamic shock where electric field is unimportant. In the general ionizing shock, an electromagnetic wave propagates ahead of the shock front. This wave gives order to the arbitrary fields ahead of the shock. The nature of this electric field is completely dependent upon the structure of the ionizing shock.

Taussig [7] has reduced this set of equations to a fourth order polynomial in u_2 where E_y has been treated as a parameter. The equation has three different roots for the $E = 0$ case, they are

$$u_2 = b_1^2/u_1$$

$$u_2 = \frac{\gamma-1}{\gamma+1} u_1 + \frac{2}{\gamma+1} \frac{a_1^2}{u_1}$$

$$u_2 = u_1.$$

The first is the switch-on shock and is a double root. The second and third are the gas dynamic and the null solution respectively. These solutions for zero electric field create a boundary for all solutions for nonzero fields.

The graph of these solutions is shown in Figure 3. M_a is the normalized velocity or Alfvén mach number, u/V_a. V_a is the Alfvén velocity given by

$$V_a = B/(\mu\rho)^{\frac{1}{2}}$$

where B is the field normal to the shock, ρ the gas density, and μ the magnetic permeability. The standard notation N, G, and SW indicate the solutions for $E \neq 0$ according to which of the $E = 0$ lines (null, gas dynamic, or switch-on) the solution lies closest.

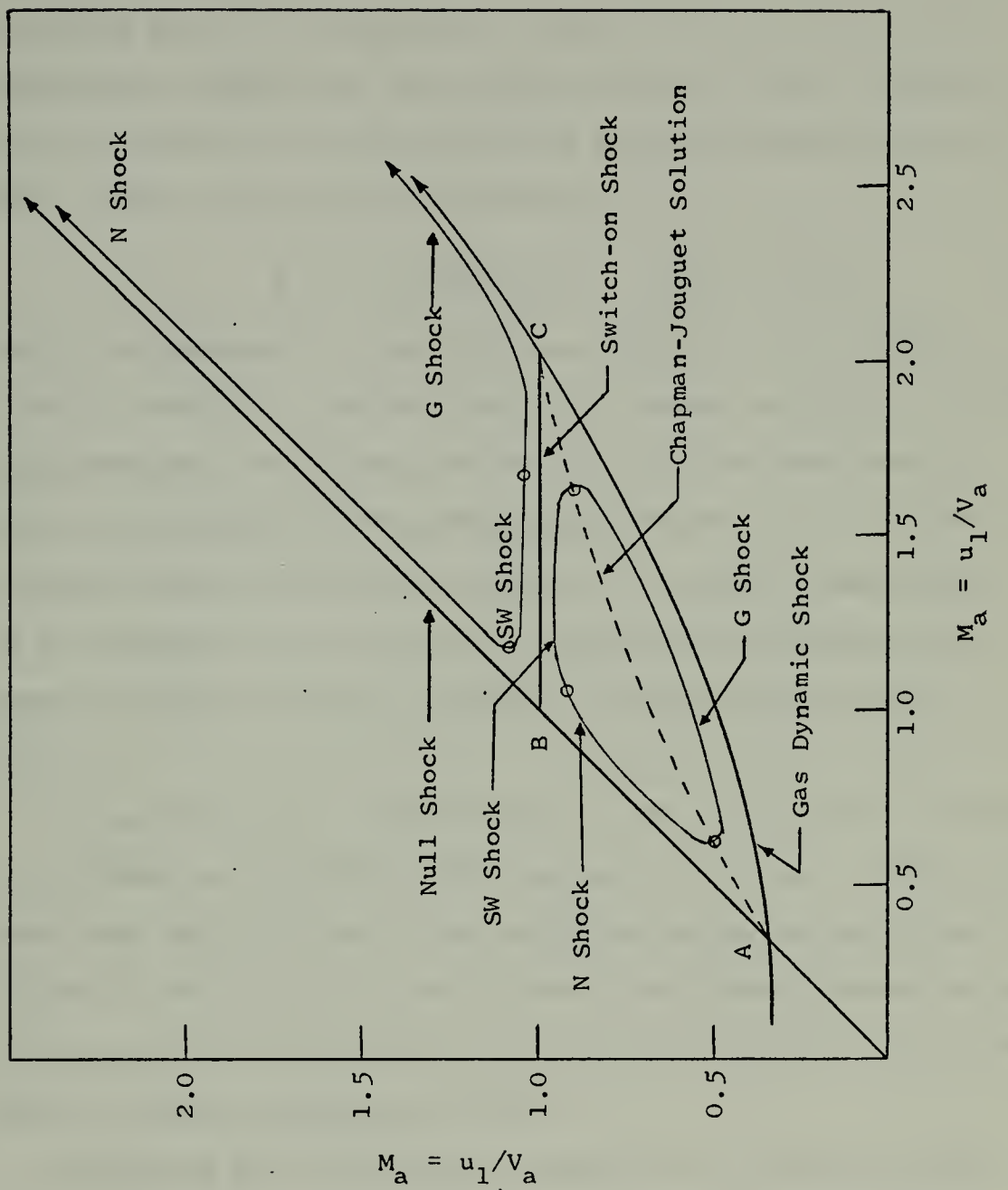

Figure 3. Typical E = 0 and E > 0 Solution Contours (from Taussig [7])

The ABC region of Figure 3 is known as the switch-on domain, and it is here that slow ionizing waves propagate. It is evident from the figure that for a given value of electric field, there is a minimum velocity below which no steady state solutions exist. Furthermore, Taussig has shown that there is a critical value of electric field, E^*, above which there exist no steady state solutions. This critical value is given by

$$E^* = 0.357(B_x^2/(\mu\rho)^{\frac{1}{2}}) \quad (\text{for } \gamma = 5/3).$$

This value represents a physical upper limit to the pre-shock electric field for a uniform post-shock plasma condition. In the electromagnetic shock tube, the value of the upstream electric field is determined by the voltage and currents involved in the breakdown and acceleration of the gas. The theory suggests that if the parameters are such that if electric field ahead of the shock exceeds the critical value, E^*, only unsteady flow can exist.

A similiar effect is encountered if the total currents flowing in the shock and rarefaction wave become very large. Taussig has shown that the solutions in the switch-on regime for which the current is too large to allow a steady state region separating the shock and drive currents are the solutions predicted by Kunkel and Gross in their hydromagnetic theory.

Kunkel and Gross based their theory upon an analogy between ionizing shocks and classical detonation waves. The chemical heating within the shock front of the detonation wave is replaced by the Joule heating which takes place within the ionizing front. The basis of detonation theory is the Chapman-Jouguet hypothesis,

and for this reason these ionizing shock solutions are referred to as Chapman-Jouguet solutions. A good discussion of the hydromagnetics of detonation and the Chapman-Jouguet hypothesis can be found in Taylor [11].

When current values reach the critical value, the distance between the shock and the current-carrying rarefaction wave has diminished to zero. This means that the two waves are no longer separated by a region of current-free, uniform plasma. Using information from the Chapman-Jouguet hypothesis, Taussig was able to solve uniquely the jump equations. These solutions correspond to the largest possible value of electric field soluble for a given shock speed. For this reason, these solutions are referred to as the extremal solutions. The work of Levine has verified this predicted behavior for switch-on waves propagating in the trans-Alfvénic region. The solution to the Chapman-Jouguet model is shown in Figure 3 as a dashed line. This mode has been verified by experimental investigations using electromagnetic shock tubes.

C. ELECTRICAL PRECURSOR EFFECTS

The existance of electrical precursors in the unshocked gas ahead of ionizing shocks is a little understood phenomenon. The nature and origin of these precursors has been examined and discussed rather thoroughly by Appleton [12], and it is from this source that the bulk of this discussion is taken. Precursor effects have not only been observed in laboratory shock tubes, but are possible explanations for certain upper atmosphere observations. In particular, radar returns from meteors and re-entry capsules indicate targets which are significantly larger than the actual

dimensions of the re-entry body. These results seem to indicate the presence of charged precursors some distance ahead of the projectile shock front.

Appleton treats three possible mechanisms which could be responsible for the formation of these effects. These are: (1) the diffusion of mobile electrons from the ionized region behind the front through and ahead of the shock; (2) photoionization of the neutral gas by ultraviolet radiation originating in the ionized region behind the front; (3) photoemission of electrons from the walls of shock tube experiments.

Appleton has constructed and solved a diffusion model for moderate strength ionizing shocks in argon. The numerical solution of the model for electron distribution and charge separation gave several interesting results. It showed the existence of a separation of charge resulting in a double layer with the maximum electric field intensity at the point where the electron density and ion density are first equal. This result indicates that the shock front is preceded by a region of high electron density which decays rapidly with distance ahead of the front. This charge separation results in the formation of an electric field within the translational front. This is followed by a region of collisional ionization downstream. This model cannot account entirely for the precursor effects observed because of the drastic decay of electron density with distance ahead of the shock.

No satisfactory theory of photoionization ahead of the shock front has yet been formulated. Existing theory cannot explain the existance of electron and ion densities which have been measured

in argon. Appleton notes, however, that the existence of even slight impurities (such as oxygen at a concentration of one part per million) can explain the inconsistant measurements.

More recent experimental investigations carried out by Lubin and Resler [13] have revealed several interesting characteristics of precursors. The precursors were found to have a wavelike structure with a sharp electron density front. The experiment, carried out using an electromagnetic T-shaped shock tube, showed that the average electron densities were dependent upon the ambient pressure. The precursor fronts were found to travel at speeds of the order of 10^8 to 10^9 cm/sec. The precursor wave was found to propagate down the tube prior to the main breakdown, as soon as high voltage was applied to the electrodes. The nature of precursors as revealed in this model cannot be explained by existing theory.

D. SHOCK STRUCTURE

Within an ionizing shock ionization is produced by two major processes. This first is ionization by atom-atom collisions, while the second is by electron-atom collisions. Chubb [14] states that the structure of such a shock in a monatomic gas can be divided into two regions according to which of the two ionization processes dominate. The initial excitation of the gas is caused by atom-atom collisions. In this first region atom-atom collisions dominate; only excitation will occur until the atoms reach a temperature large enough to produce significant ionization. Ionization continues until its rate becomes greater than the recombination rate. At this point the more efficient electron-atom ionization process begins and soon dominates.

The first region is called the viscous shock region, as viscous atom-atom dissipation effects dominate. The thickness of the first region is the order of the atom-atom collisional mean free path. The second region known as the relaxation zone. Here most of the ionization occurs and its dominant mechanism is electron-atom collisional processes. The thickness of the relaxation zone is dependent upon the ratio of the electron mass to the atomic mass and the electron-atom collisional mean free path.

E. SWITCH-ON CHARACTERISTICS

In magnetohydrodynamics a switch-on shock is one in which the preshock state is characterized by no transverse magnetic field and no transverse momentum, but in whose postshock state these quantities are non-zero. Slow ionizing waves which are preceded by an electric field possess these characteristics. The transverse magnetic field and momentum are switched on by the passage of the ionizing front. These postshock conditions are the result of current flowing through the shock wave structure. According to Gross [15] the appearance and disappearance of the switch-on behavior of the waves is dependent upon the stability of the wave. There has not been a conclusive analysis of the stability of normal ionizing shock waves.

F. SPECTROSCOPIC LINE INTENSITY METHODS

A time resolved spectroscopic investigation of the optical radiation associated with the ionizing shock wave was desired. For this purpose, modification of the pinch-discharge system allowed for the attachment of a Beckman and Whitley time resolving

spectrograph equipment group. This group consists of a model D-2 Dispersion unit and the model 339 continuous writing streak camera. In such a time resolved spectrum, the presence or absence of certain spectral lines can give a clearer picture of the mechanisms involved in the dissipation of energy across the front. Line intensity measurements can give additional qualitative diagnostic information such as effective temperatures and densities.

The absolute intensity of a spectral line is given by Robinson and Lenn [16] as

$$I_{mn} = \left[A_{mn}(E_m - E_n)g_m N/Q \right] \quad \exp\ (-E_m/kT_e)$$

where

A_{mn} = transition probability in sec^{-1}

E_m, E_n = energies in joules of the upper and lower states of the transition respectively

g_m = statistical weight of the upper state

N = number density of the species in m^{-3}

Q = internal partition function or state sum of the species

T_e = effective temperature in degrees Kelvin

In many instances the intensity is written in terms of the oscillator strength, f.

$$f_{mn} = 1.5 \times 10^{-16}\ \lambda^2\ A_{mn}$$

where λ is the wavelength of the transition and f_{mn} and A_{mn} are determined by quantum mechanical calculations. The absolute intensity then becomes

$$I_{mn} = 13.2(f_{mn} g_{mn} N/\lambda^3 Q)\ \exp\ (-E_m/kT_e).$$

Tabulation of oscillator strength values for Argon and other elements can be found in Griem [17].

The relationship between the effective temperature (excitation temperature) indicated by line intensity measurements and the kinetic temperature of the electrons, ions, and neutrals depends upon the collisional situation in the plasma. Excitation leading to radiation may be caused by collisional processes among the particles, by the absorption of radiation, or by instability phenomena. In many cases, the velocity distributions of electrons, atoms, and ions, as well as their degree of excitation and ionization, may be very close to those of a system in thermodynamic equilibrium. In such situations the system is said to be in local thermodynamic equilibrium (LTE), which can exist if collisional processes dominate radiative processes. In a shock wave, LTE would not be expected within the shock front itself. However, in most cases the decaying plasma in the postshock state will meet the requirements of local thermodynamic equilibrium. Equilibration times and procedures for LTE evaluation for shock tubes are given by Griem [17].

The line ratio technique makes it possible to determine effective temperature without measurement of absolute line intensities. For a single species the values of the number density, N, and the internal partition function, Q, are identical for any two lines and therefore drop from the ratio of intensities. This eliminates the necessity of knowing the pressure to determine the temperature. For a dual line ratio, the expression for kT_e may be

written

$$kT_e = \frac{E_{m1} - E_{m2}}{\ell n(I_1/I_2) - \ell n(g_1A_1\nu_1/g_2A_2\nu_2)}.$$

If more than two lines are used increased accuracy in temperature determination can be obtained. Taking the logarithm of both sides of the absolute Intensity equation leads to

$$\ell n(I_{mn}\lambda^3 Q/f_{mn}g_m) = \ell n(13.2N) - (E_m/kT_e).$$

The graph of $\ell n(I_{mn}\lambda^3 Q/f_{mn}g_{mn})$ as a function of E_m will be a straight line with slope $-1/kT_e$ and intercept $\ell n(13.2N)$. If the graph does not yield a straight line the plasma is not in local thermodynamic equilibrium.

IV. EXPERIMENTAL PROCEDURES

A. MODIFICATION OF THE THETA PINCH SYSTEM

At the commencement of this study, it was determined that certain modifications to the system of Christensen [2] would be necessary. The previous arrangement included an array of six oil-filled 7.0 microfarad capacitors situated with the electrode face in a vertical position. This face was the top of the oil container, having rubberized seals to prevent oil leakage. The positioning of the capacitors on their sides resulted in oil contact with the seals. This apparently led to deterioration of the seals with subsequent oil leakage from the capacitors.

It was determined that the system should be modified such that these large capacitors would be oriented to prevent further leakage. The present configuration of the capacitor bank incorporates this proper positioning of the capacitors with easy access to the plasma column. This allowed for attachment of the time-resolving spectrograph unit and would be suitable for installation of other diagnostic equipment, such as the plasma spectrophotometer, above the capacitor bank.

The modification of the capacitor bank required only minor alteration of the discharge system and resulted in negligible change in the inductance of the discharge circuit. The only modification to the discharge system resulted from a necessary change in the orientation of the pressurized spark gaps with respect to the fast discharge capacitors. The change involved the insertion

of a 90 degree elbow between the positive electrode of the capacitor and the high voltage lead of the spark gap. Only minor alterations to the previous spark gap design were necessary to accommodate the new connector.

B. INSTALLATION OF THE SPECTROGRAPH

The capacitor bank modifications specifically allowed for the attachment of the spectrograph unit. The unit was installed adjacent to the first port downstream of the theta pinch coil, a distance of 28.5 cm. The camera and dispersion unit were aligned and focused, being linked to the system by an opaque light tube. The dispersion unit has a minimum focal distance of six feet, and can be adjusted to image objects out to infinity upon the spectral slit. The camera was for this reason positioned a distance slightly greater than six feet from the center of the plasma column. The position of the spectrographic unit relative to other system components can be seen in Figure 4.

C. PHOTOELECTRIC DETECTION

Observations of the luminous front associated with the ionizing shock were performed using photomultiplier detection equipment. Two RCA 5819 photomultipliers mounted in Orion housings were used. These were fitted with a dual lens system which allows focusing upon the column center minimizing the amount of stray light pick-up. These photomultipliers were located at ports 28.5 cm and 63.5 cm downstream of the theta pinch coil edge.

Additional observations were made using an RCA 1P21 photo-multiplier tube in a Quanta housing. This photomultiplier package

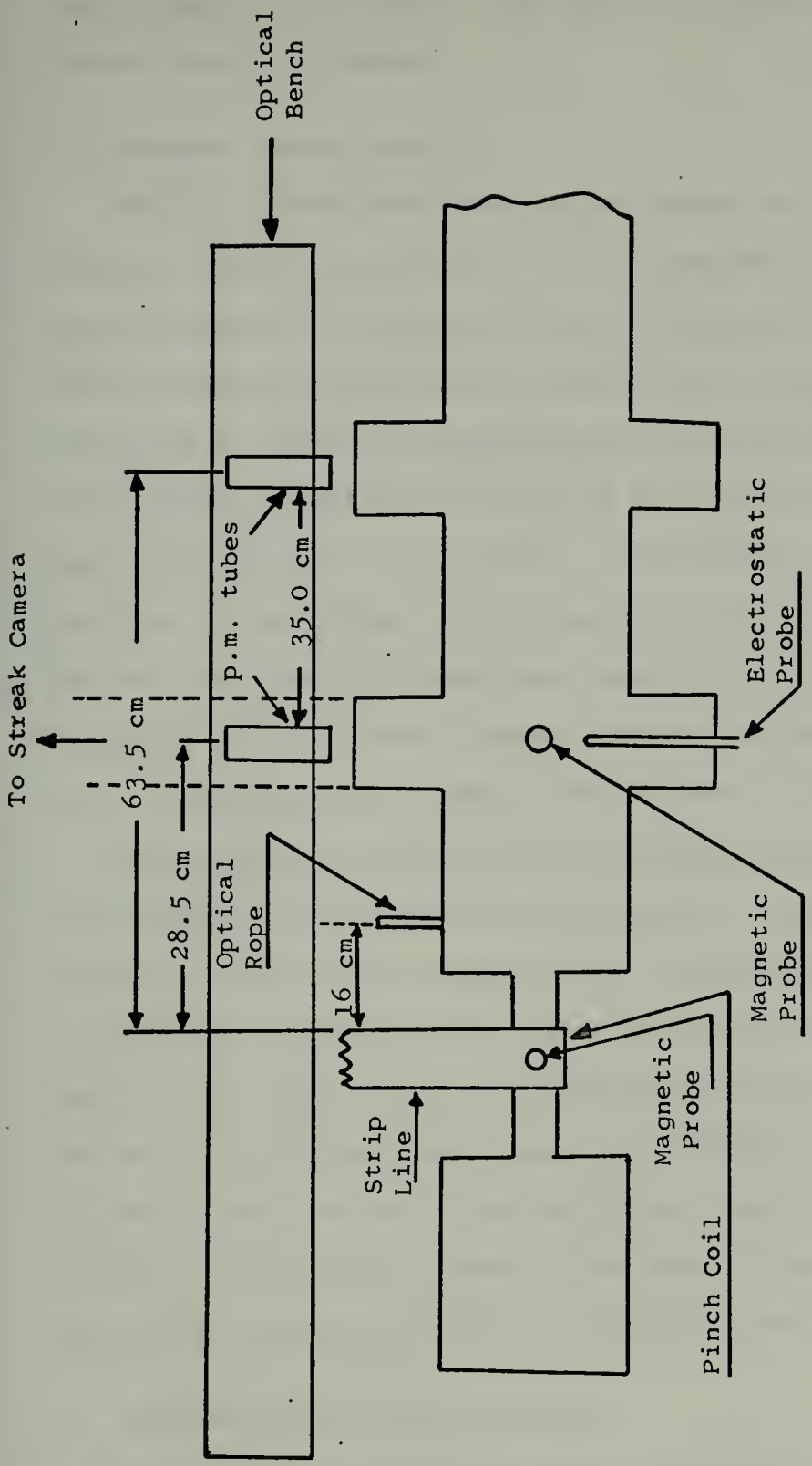

Figure 4. Location of Diagnostic Equipment

was fitted with an optical rope which allowed observation at various points along the column.

D. MAGNETIC PROBE DETECTION

Magnetic probes were utilized to detect and measure transient magnetic fields associated with the propagating shock and the theta pinch discharge. A magnetic probe is essentially an inductive coil which produces an electrical signal which is proportional to the time rate of change of magnetic flux through the coil. The probes used in this investigation had coil areas of the order of one square mm and from 5 to 10 turns. By changing the orientation and position of the probes the various components of the transient magnetic field may be selectively measured. A more complete description of the magnetic probes used at the plasma facility as well as calibration procedures may be found in McLaughlin [18].

Probe output was displayed on a Tektronix type 555 dual beam oscilloscope. The scope was equipped with a type "O" operational amplifier plug-in unit which allows integration of the input signal. The operational amplifier has a variable RC time constant capability. Best results were obtained when the time constant was set at 5 to 10 times the frequency of the input signal. The oscilloscope was located in an isolating screen room. Signals were relayed to the scope by means of shielded 50 ohm characteristic impedence terminated coaxial transmission line.

E. ELECTROSTATIC PROBE DETECTION

Electrostatic probes were used in the investigation to aid in detection and study of the ionizing fronts. The probes were of the

single point type and were used only for detection of the presence of charged particles, ie. the onset of ionization. The probe output was displayed on the Tektronix type 555 oscilloscope described in the above section.

V. RESULTS

A. OBSERVATION OF THE SHOCK FRONT

Detection of the shock front was realized by use of photomultipliers and electrostatic probes. Photomultipliers were employed for observation of the luminous front while the electrostatic probes were used to detect the occurrence of ionization. Descriptions of these devices may be found in the previous chapter on experimental methods.

Display of these signals on a dual beam oscilloscope revealed that there was a separation between the luminous front and the onset of ionization. Figure 5a shows a typical example of the two traces. The upper trace is the electrostatic probe signal and the lower is the photomultiplier signal. This particular oscillogram was taken with a charging voltage of 15 kV, initial pressure of 100 m Torr, and a steady state magnetic field of 4800 gauss. The time scale is 20 microseconds per division with time proceeding from right to left. The luminous front precedes the ionization front by approximately 22 μsec.

Using an estimate of front velocity of 2.38 km/sec a separation distance of 5.24 cm results for the above example. The separation distance was found to increase with increasing pressure. For similar conditions at a pressure of 100 m Torr the separation was calculated as 13.0 cm.

Figure 5a.

Upper Trace: Electrostatic Probe

Lower Trace: Photomultiplier

28.5 cm downstream

20 μsec/div

B = 4800 Gauss

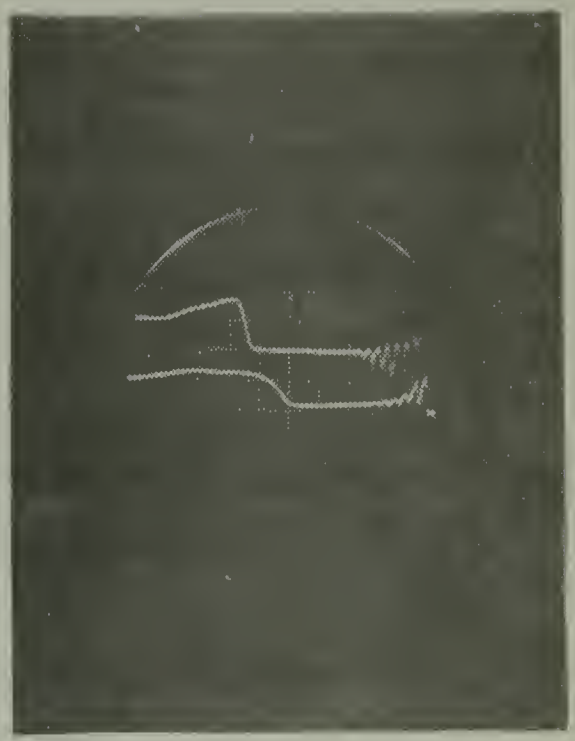

Figure 5b.

Upper Trace: Photomultiplier

20 μsec/div

28.5 cm downstream

Lower Trace: Magnetic Probe

Integrated signal of probe located in center of θ-pinch region

2 μsec/div

B = 3600 Gauss

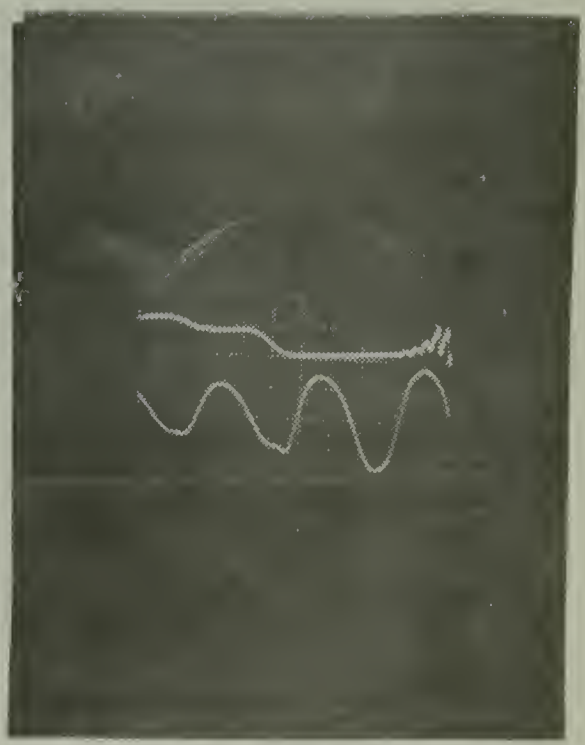

Figure 5. Photomultiplier, Magnetic Probe, and Electrostatic Probe Signals

The width of the luminous front can be estimated from the rise time of the photomultiplier signal in a manner similar to the calculations above. For the example shown in Figure 5a, the rise time is less than the separation time between the two fronts. The corresponding shock width is 2.38 cm. Unlike the aforementioned separation distance, the width associated with the luminous front decreases slightly with increasing pressure. The width for the 1000 m Torr pressure is 2.04 cm.

A second rise in the photomultiplier signal was observed to follow the first. A clear example of this effect is shown in Figure 5b, where the upper trace is the photomultiplier using a time scale from right to left of 20 μsec per division. The lower trace shows the magnetic field rise within the pinch, and correlation of the two signals is not intended.

In this case the second rise in radiation occurs approximately 40 μsec after the first. This is approximately 10 to 15 μsec after the onset of ionization.

B. PARAMETRIC VARIATION OF LUMINOUS FRONT VELOCITY

Velocities of luminous fronts associated with ionizing shock-waves were determined using the photoelectric detectors discussed in the previous chapter. The initial rise of magnetic field in the pinch coil as detected by magnetic probes was used as a zero-time reference and as an oscilloscope trigger.

It was found that the radiation loss in the optical rope was very significant and that an oil film on the inside of the glass column presented a similar problem. As a result, the number of points along the column at which this photomultiplier assembly

could be used was severely limited. The arrival of the luminous front was consistently detected at only three points along the column, the two ports downstream and a position 16.0 cm from the edge of the pinch coil.

This limited number of points made accurate determination of the front velocity by graphical differentiation of distance versus time curves quite difficult. For this reason mean velocities between the points in question were used. These were calculated by simply dividing the distance travelled by the time of travel, and are not to be interpreted as instantaneous velocities.

1. Variation of Velocity with Initial Pressure

Time of arrival of the luminous front as a function of the initial gas pressure was determined as described above. These measurements were made using the photomultiplier located at the first port, 28.5 cm downstream of the coil edge. The times were converted to mean velocities using the method described above. The results are shown graphically in Figure 6. At pressures below 30μ the arrival of the luminous front could not be detected. Logarithmic graphical analysis of these data for the steady state field of 4200 gauss gave the following relationship between mean velocity and initial pressure.

$$\bar{v} = 7.15\, p^{-0.17}$$

The graphical relationship of log $\bar{v}$ versus log p is shown in Figure 7. The error bars represent estimated uncertainty in both velocity and pressure measurements.

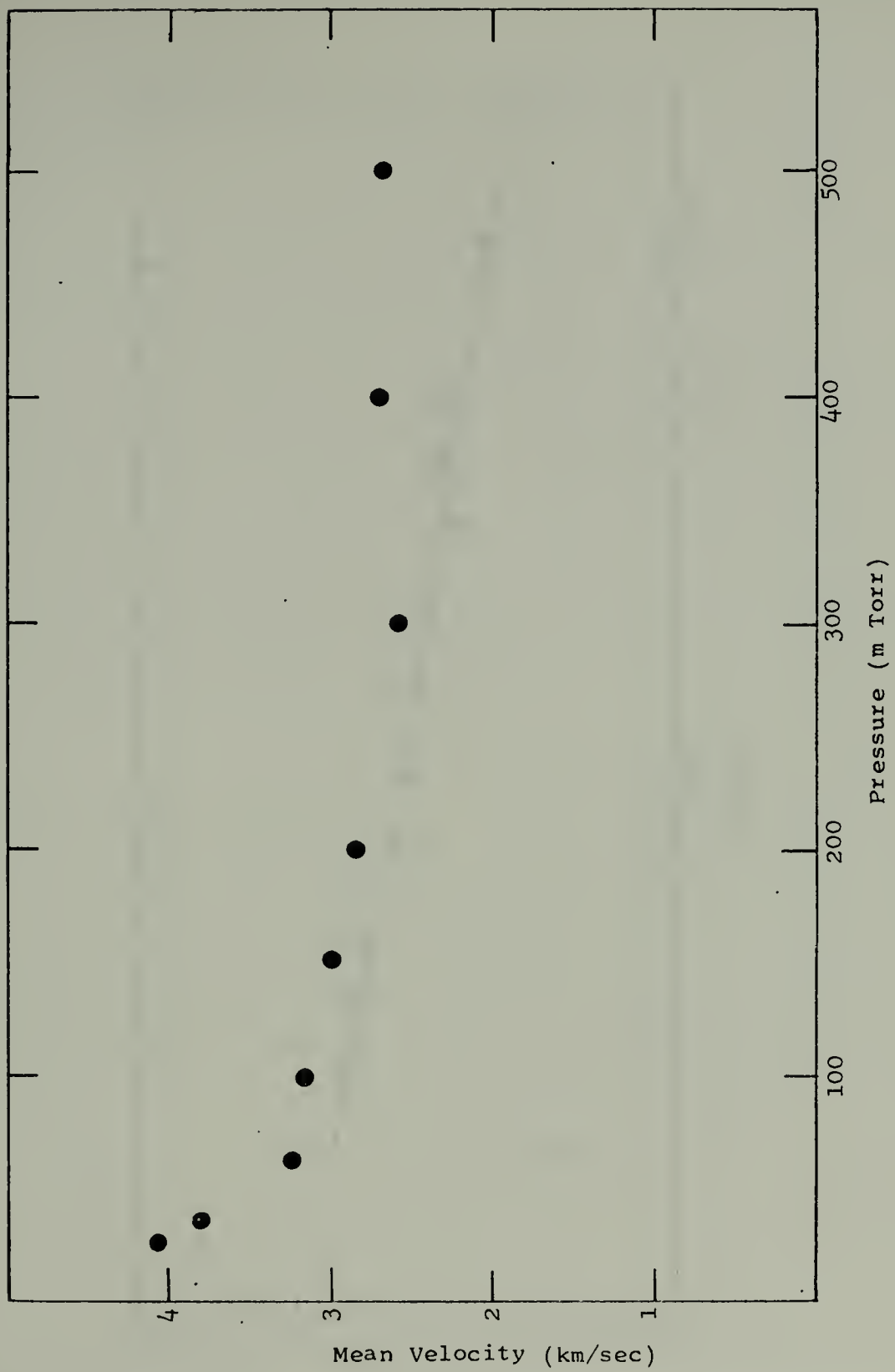

Figure 6. Mean Velocity Versus Initial Pressure for 0.285 m Downstream

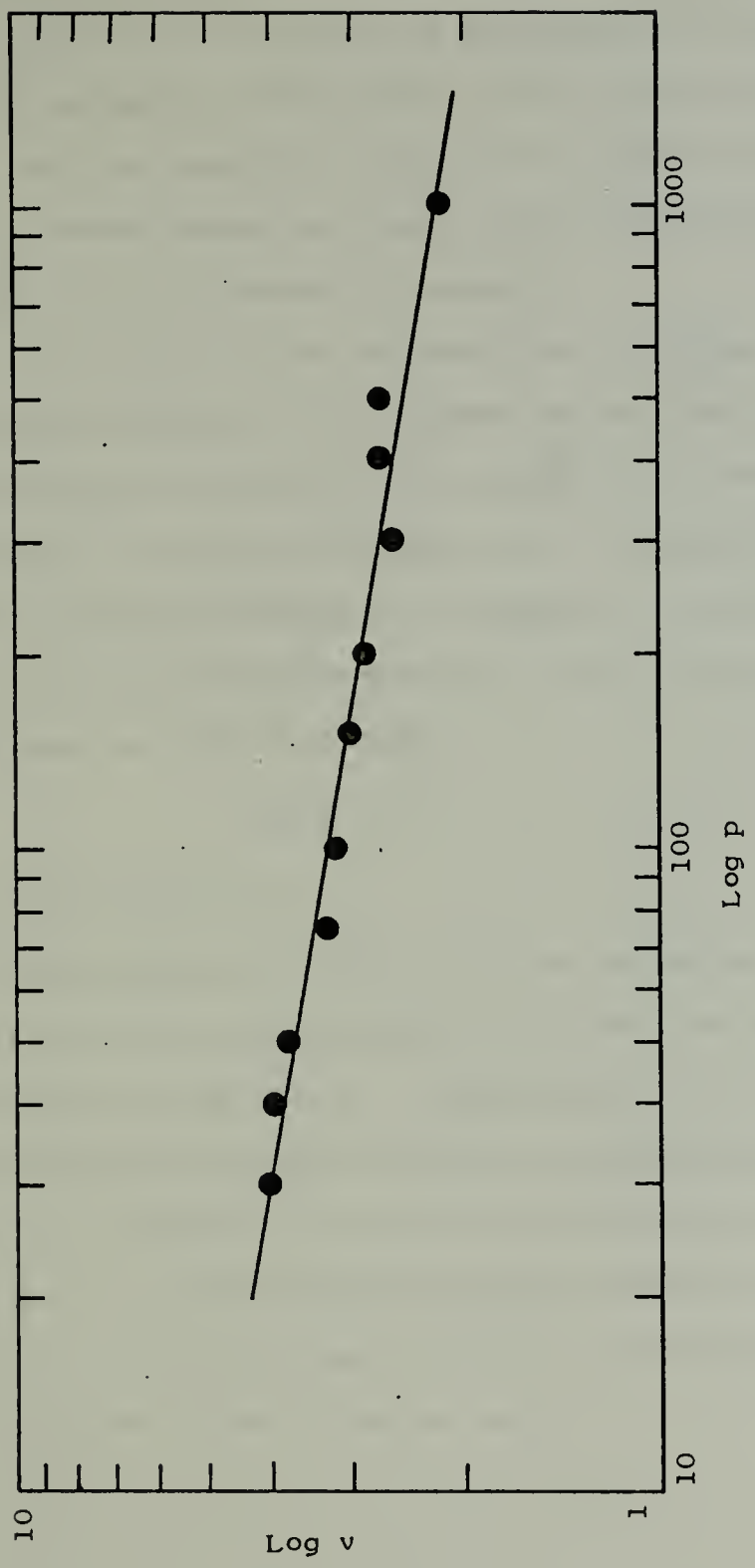

Figure 7. Log v Versus Log p for 28.5 cm Downstream

2. Variation of Velocity with Steady State Magnetic Field

The effect of a steady state magnetic field longitudinally directed and normal to the plane of the shock front was experimentally investigated. Measurements of mean velocities of the luminous front were made with values of the normal field up to 7200 gauss. Measurements were made at the three positions discussed above using photoelectric detectors.

The variation of mean velocity for a position 0.285 m downstream with magnetic field is shown graphically in Figure 8. These measurements were taken with an initial gas pressure of 100 m Torr and a charging voltage of 15 kV. Graphical analysis using full logarithmic scales gave an empirical relationship between velocity and magnetic field for field strengths greater than 1800 gauss as indicated below.

$$\bar{v} \alpha B^{-0.29}$$

This is shown in Figure 9.

The dependence of mean velocity on the magnetic field strength for positions 16 cm and 63.5 cm downstream are shown in Figures 10 and 11 respectively. Qualitatively these results indicate that the average velocity between the pinch coil and 16 cm decreases with increasing magnetic field strength while the average velocity to 63.5 cm downstream of the coil increases with increasing field. Possible explanations for this unusual behavior will be discussed in the following chapter.

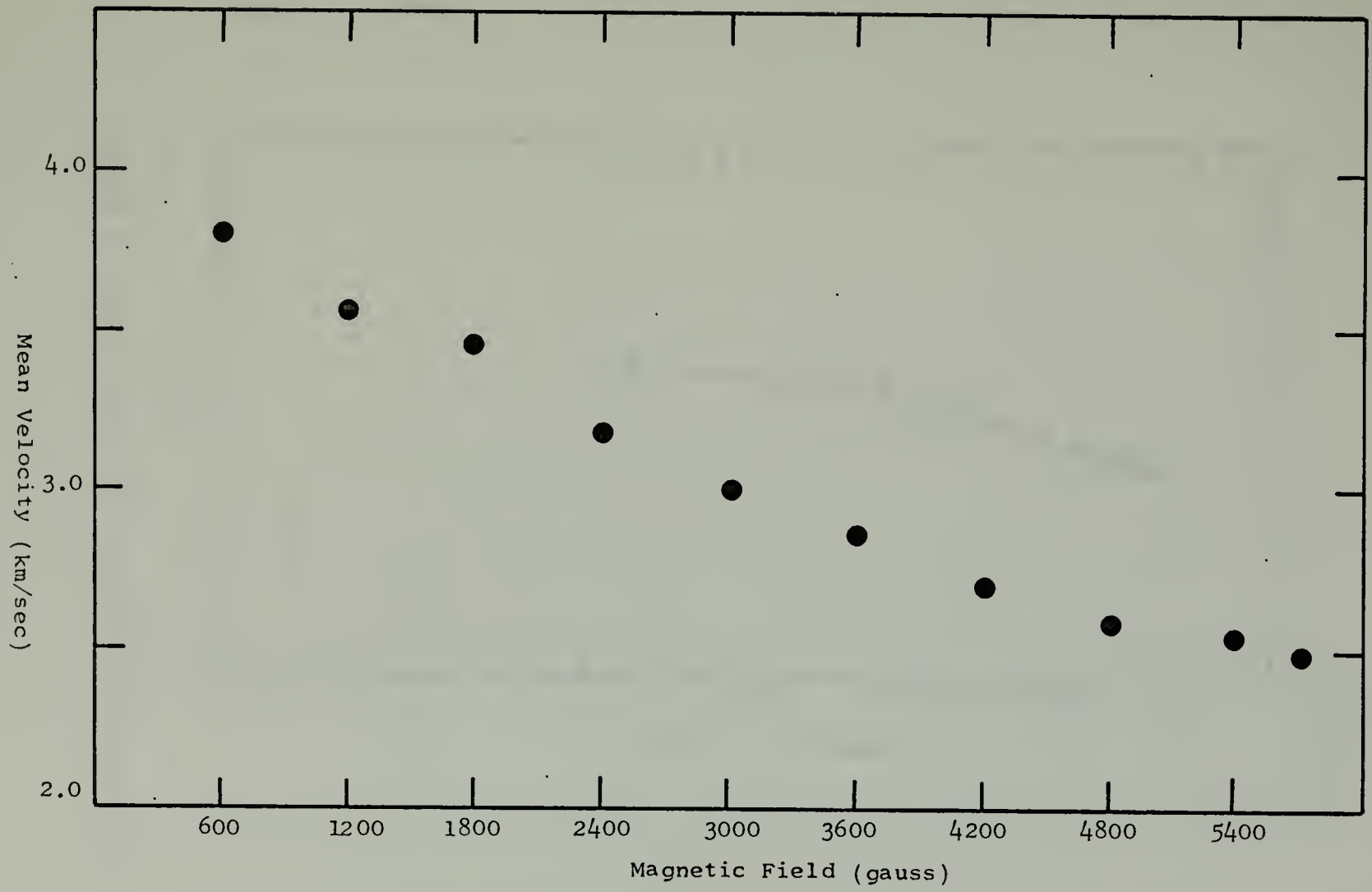

Figure 8. Mean Velocity Versus Magnetic Field for 28.5 cm Downstream

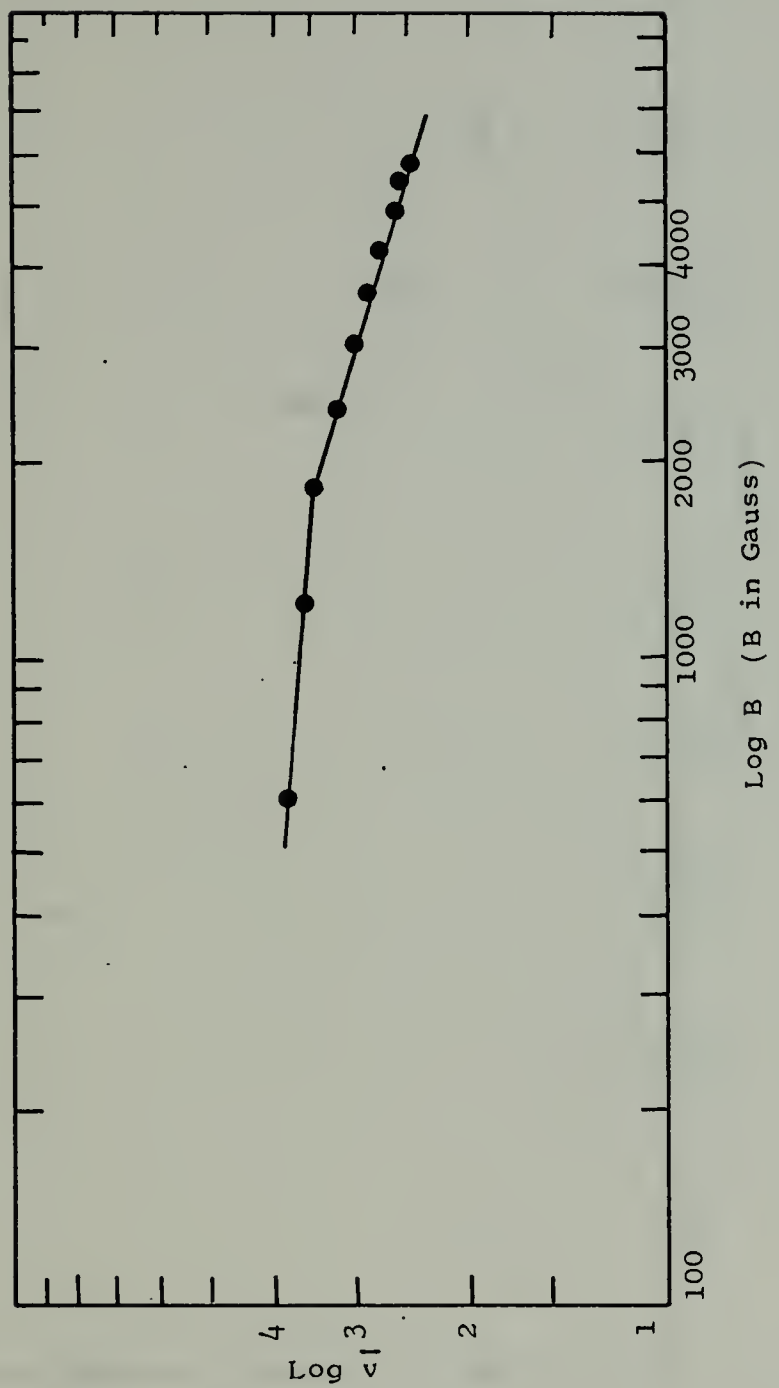

Figure 9. Log $\bar{v}$ Versus Log B for 28.5 cm Downstream

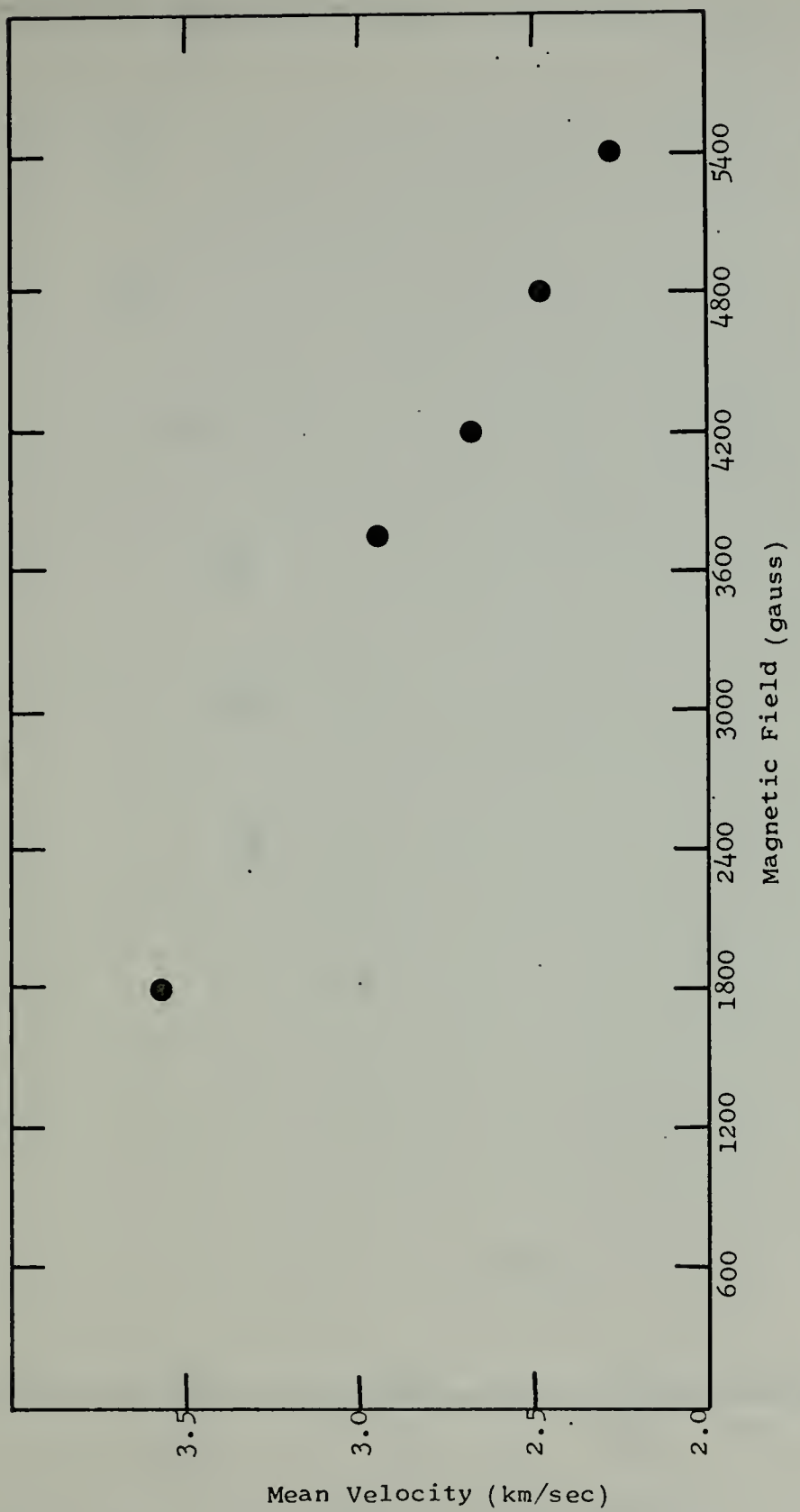

Figure 10. Mean Velocity Versus Magnetic Field for 16 cm Downstream

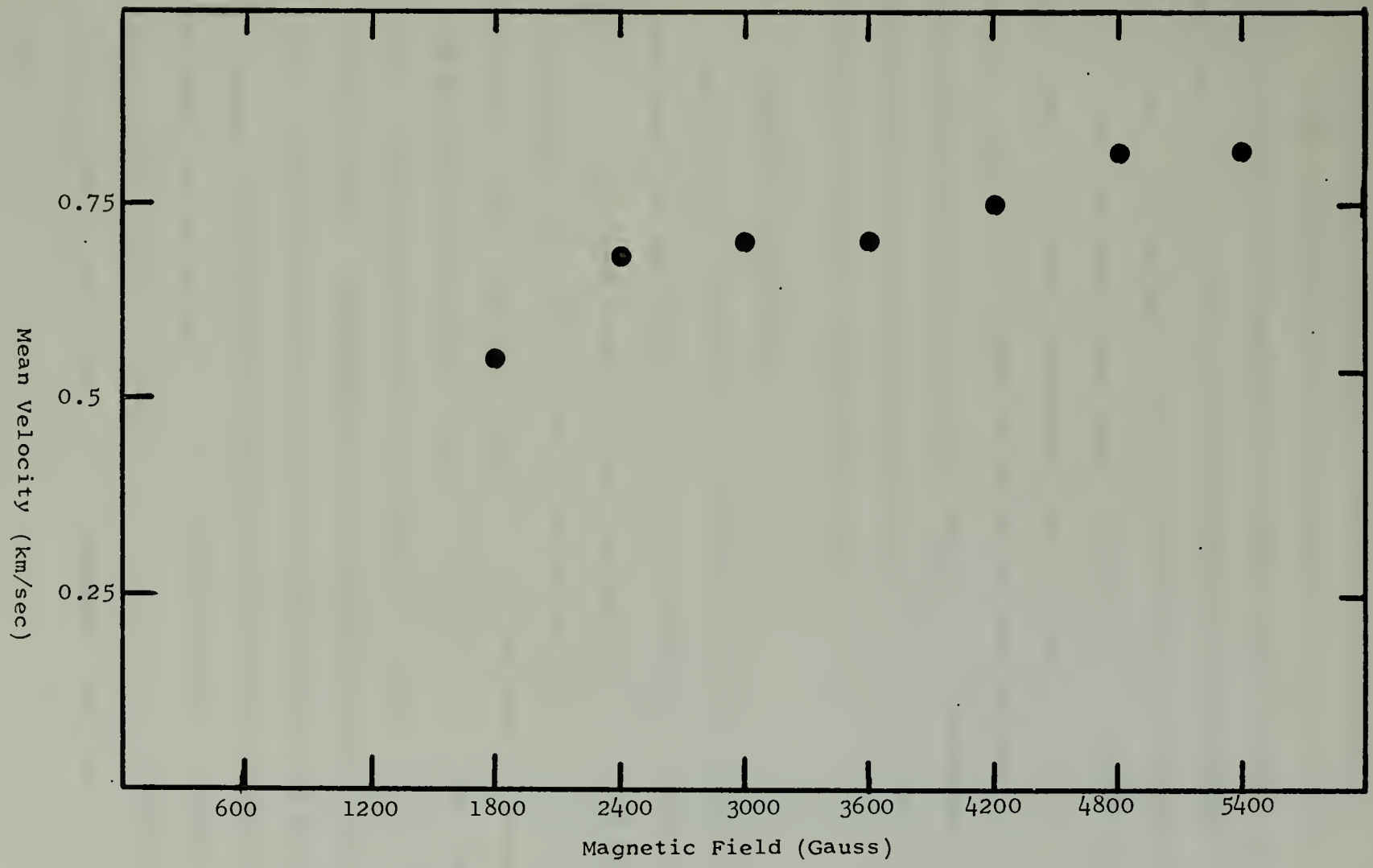

Figure 11. Velocity Versus Magnetic Field Strength for 0.635 m Downstream

3. Variation of Velocity with Capacitor Bank Voltage

The time of arrival of the luminous front for various charging voltages was measured in a manner similar to that described above. The value of bank voltage was varied between 10 and 20 kV. The luminous front was not observed for voltages less than 10 kV. The results are shown in Figure 12. The mean velocity was shown to be linearly dependent upon voltage up to 17.5 kV. The velocity appears to decrease for values of bank voltage in the 20 kV range. The measurements were taken 28.5 cm downstream of the pinch coil with an initial gas pressure of 100 m Torr, and a steady state axial magnetic field of 3600 gauss.

C. PRECURSOR OBSERVATIONS

Fast precursor radiation was detected downstream of the theta pinch using photomultipliers. A sample oscillogram is shown in Figure 13. The time scale is 20 microseconds per division and time proceeds from left to right. The initial rise in the photomultiplier signal (top trace) appears at approximately the same time as the initial magnetic field rise in the pinch area (lower trace). The photomultiplier is located 28.5 cm downstream of the pinch coil edge. Superimposed upon the photomultiplier signal is a small amount of electrostatic pick-up generated by the capacitor discharge. This electrostatic noise hindered the determination of the exact time of arrival of the precursor radiation. The precursor does arrive on the same time scale as the pinch discharge when compared to the arrival of the luminous front some 110 μsec later.

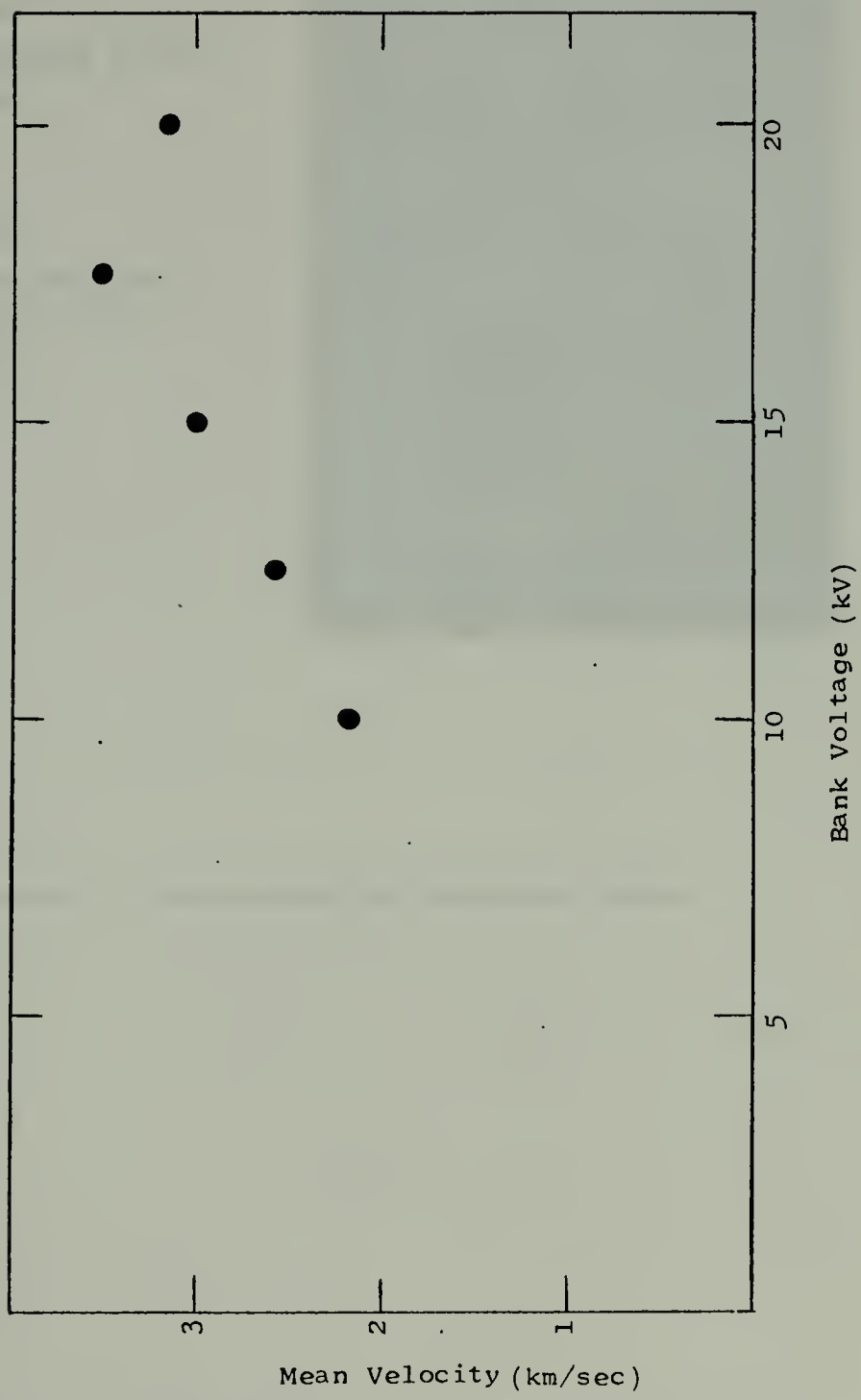

Figure 12. Velocity Versus Bank Voltage for 0.285 m Downstream

Upper Trace:

Photomultiplier Signal

20 μsec/div

.2 v/div

Lower Trace:

Magnetic Probe Signal within Theta Pinch

20 μsec/div

.05 v/div

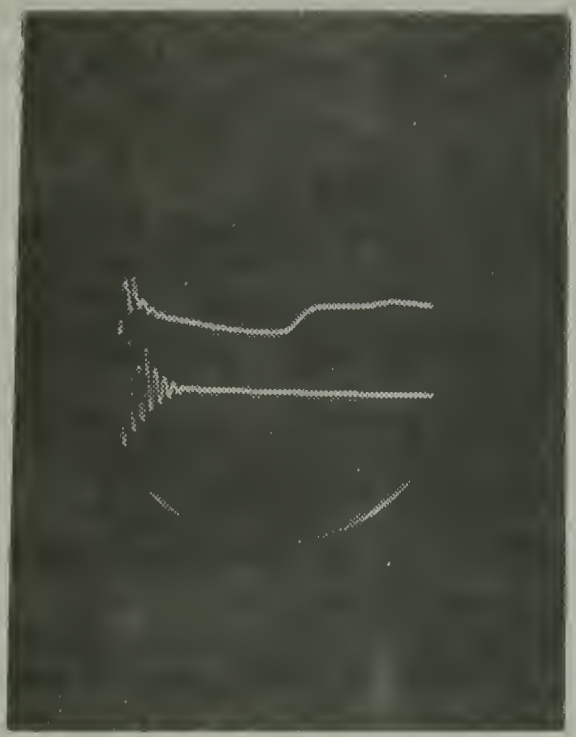

Figure 13. Photomultiplier Precursor Signal

Detection of charged particles downstream using electrostatic probes requires sensitivity increased over that needed for the photomultiplier. For this reason signals indicating the possible presence of charged species were masked by electrostatic pick-up due to the discharge.

D. OBSERVATION OF HIGH MAGNETIC FIELD CUTOFF

A maximum value of steady state magnetic field was observed above which no luminous front was seen. For a capacitor bank voltage of 15 kV the cutoff field was found to be 6000 gauss. For steady-state fields equal to or greater than 6000 gauss observations of radiation downstream of the pinch revealed no evidence of shock front formation. There was no evidence of either precursor radiation or shock radiation. For values of magnetic field slightly less than 6000 gauss no unusual effects were observed.

For a charging voltage of 20 kV similar results were observed, but with a cutoff field of 7200 gauss. The cutoff value for 10 kV was 4200 gauss.

E. OBSERVATION OF TANGENTIAL MAGNETIC FIELD VARIATIONS WITHIN THE SHOCK

Magnetic probe measurements of the tangential components of magnetic field across the shock were made to confirm the switch-on behavior of the shock. The measurements were conducted using 10-turn magnetic probes located 28.5 cm downstream of the pinch coil. To date no change in magnetic field across the shock has been detected.

F. RESULTS OF SPECTROSCOPIC OBSERVATIONS

Attempts to produce time resolved spectral pictures of the luminous fronts were unsuccessful. Runs taken with the camera mirror in a static position failed to produce any results on film. These results can be attributed to the fact that with the camera in its present configuration and using low gas pressures, the luminescence intensity of the gas is not sufficient to overcome the losses encountered in the dispersion unit.

VI. DISCUSSION OF RESULTS

Results of photomultiplier and electrostatic probe investigations of the shock revealed that the ionization front was preceded by a luminous front. The theory of the structure of ionizing shocks in a monatomic gas predicts such a two region shock with a viscous region thickness the order of the atom-atom mean free path. The collisional mean free path for atom-atom interaction in argon at 100 m Torr can be taken as 0.021 cm. The separation distance between the two fronts found in this study was calculated as 5.24 cm, two orders of magnitude larger. This result seems to indicate that the nature of the two fronts produced at the plasma facility is considerably different from that of the standard ionizing shock.

The behavior of the separation distance between the two fronts with increasing initial pressure is opposite to that which would be expected if the process were dominated by atom-atom collisional processes. The separation distance increases with increasing pressure, while the collisional mean free path decreases. This effect seems to eliminate the possibility of ionization occurring when a critical temperature is reached within the viscous region. The result leaves open the possibility that the two fronts are in fact two separate disturbances propagating separately, the second being created at some time after the first.

The observations of the effect of steady state magnetic field on shock velocity indicate that at least two separate effects are being observed. Observations closest to the pinch coil indicate

a decrease in velocity with increasing magnetic field, while farther downstream the velocity increases with increasing field. This leads to the conclusion that the increased field tends to result in a decrease in the initial velocity of the shock. Results downstream can be explained in terms of dissipative effects. The increase in magnetic field acts to deter dissipation of the wave as it propagates downstream. The field can be thought of as a confining duct which prevents radial drift of charged particles and consequent loss of energy. This result indicates that the luminous front is somehow related to the ionization front. If the luminous front were a separately propagating gas dynamic shock, no magnetic field interaction would be expected.

Observations at all points downstream of the theta pinch coil must therefore include the effect of the initial velocity as well as dissipative mechanisms. Separation of the two effects has not been attempted in this study. The variation of mean velocity to the first port (28.5 cm downstream) with initial pressure, capacitor discharge voltage, and steady state magnetic field is given by the following empirical relation,

$$\bar{v} = A\, p^{-0.17}\, B^{-0.29}\, V$$

where A is a constant depending upon other factors. This relation is good only for fields greater than 1800 gauss.

The observation of high magnetic field cut-off discussed in the previous chapter is not well understood. It is the opinion of the author that this result as well as velocity variations may possibly be explained in terms of magnetic pressure and the trapped field. The operation of the theta pinch may be explained in terms

of magnetic pressure. When the plasma within the coil excludes the diffusion of the field a large magnetic pressure external to the plasma acts to compress the plasma until a magnetostatic pressure balance is obtained. The equation governing this pressure balance is

$$p + B^2/8\pi = \text{const.}$$

where p is the kinetic pressure of the plasma and $B^2/8\pi$ is the magnetic pressure.

Considering the discontinuity between the excluded magnetic field and the plasma the equation becomes

$$B_1^2/8\pi = p_2 + B_2^2/8\pi .$$

Where the region of the excluded field is subscripted 1 and assumed to contain no particles while region 2 contains the plasma with pressure p and magnetic field B_2. Compression of the plasma will proceed until this pressure balance is reached.

When the Pinch coil is discharged with a neutral gas within it. the field will diffuse into the gas until such time that ionization takes place, and diffusion is retarded. When the gas reaches a state of conductivity such that diffusion of the field is slight, any further increase in the field due to current flow through the pinch coil will act as a magnetic piston and will compress the plasma until the magnetostatic pressure balance condition is met. The magnetic field, which has diffused into the gas before the high conductivity inhibits further diffusion, will be trapped within the plasma region and contribute a magnetic pressure. In the case of a steady state field present before pinch discharge,

the plasma field, B_2, will include both the trapped steady field and the trapped perturbation field.

$$B_2 = B_0 + B_p$$

where B_0 is the steady state field and B_p is the diffused trapped perturbation field.

Using this model it is evident that the pressure at which the equilibrium condition is reached is highly dependent upon the value of B_2. For a given value of the perturbation or pinch field the value of the trapped perturbation field will remain constant depending only upon the ionization time. Variation of the steady field, B_0 will result in a change in the value of equilibrium pressure p_2. An increase in B_0 will cause a decrease in p_2. Such a decrease will mean a decrease in the axial pressure gradient at the edge of the theta pinch coil. As was mentioned in the previous chapter dealing with the theory of the shocks, this pressure gradient is possibly the mechanism by which the shock is generated. It would therefore be expected that a decrease in the gradient caused by an increase in B_0 would be reflected in a decrease in the initial shock velocity. Such a decrease has been observed in this investigation.

The apparent cutoff of luminous shocks may be interpreted in a similar fashion. At the cutoff field the resulting value of p_2 may be so small that the energy contained within the discontinuity is not sufficient to cause luminosity as the front propagates downstream. A decrease in the capacitor voltage results in a decrease in the peak value of the perturbation field. Such a decrease would

be expected to result in a smaller value of B_0 necessary to cause cutoff. Such behavior has been qualitatively observed in this investigation.

VII. CONCLUSIONS

Normal ionizing shocks in neutral argon gas have been generated using a cylindrical theta pinch device. Propagation and structure of these shock waves has been investigated using photoelectric detectors, magnetic probes and electrostatic probes. Time resolved spectroscopic investigations were attempted but were unsuccessful due to insufficient luminosity associated with the shock front.

Investigations of front velocity with varied values of steady state magnetic field strength indicate that two interaction effects influence the downstream shock velocity. The first effect appears to be associated with the generation phase, where increases in the field result in decreases in initial shock velocity. A magnetostatic pressure balance model of the pinch generation phase formulated by the author seems to give a qualitative explanation of this effect. The second interaction involves the deceleration of the front as it propagates downstream. The steady state magnetic field appears to create an anisotropy which results in a decrease in energy dissipation with an increase in field strength.

A high field cutoff was observed in which no luminous shock propagated with steady state magnetic field above a certain value. This cutoff effect appears to be related to the shock generation field effect mentioned above and can be partially explained by the magnetostatic pressure balance model.

The importance of initial pressure to the shock wave propagation velocity was investigated. Measurements of velocity for pressures between 20 m Torr and 1 Torr indicate a decrease in velocity with increasing pressure.

Electrostatic probe studies indicate that the luminous front is followed by an ionization front ahead of which ionization is negligible. The two fronts appear to be separated by a distance several orders of magnitude large than the atom-atom collisional mean free path. Magnetic probe investigation failed to indicate any switch-on behavior associated with the shock.

APPENDIX A

TIME RESOLVED SPECTROGRAPH SPECIFICATIONS

Objective Lens: Low magnification reflection optics

Object Distance	Magnification	Aperture Ratio
500 cm	0.10	f/4.2
250 cm	0.20	f/4.3
160 cm	0.30	f/4.8

Collimating Optics: 16 inch focal length f/4 parabolic aluminized mirror

Dispersion Device: Plane reflectance grating 102 x 127 mm

Ruling: 150/mm

Central Wavelength: 6000 Å

Field 4.50 Å

Spectral Resolution on film: 4.1 Å

Collecting Optics: 16 inch f/4 parabolic mirror, 1 in. field

Entrance Slit: Variable from 0.02 to 3.0 mm

Wavelength Calibration: Low pressure mercury vapor lamp

REFERENCES

1. D.M. Budzik, Construction of a Theta-Pinch for the Generation of Shock Waves in a Nitrogen Plasma, Naval Postgraduate School Thesis, (1970).

2. C.L. Christensen, Investigation of Theta-Pinch Produced Shock Waves in a Plasma, Naval Postgraduate School Thesis, (1971).

3. R.C. Andrews, Shock Production, Langmiur Probe Diagnostics, and Instabilities in a Nitrogen Plasma, Naval Postgraduate School Thesis, (1968).

4. J.C. Beam, Investigations in the Vacuum Ultraviolet of a Steady State Nitrogen Plasma, Naval Postgraduate School Thesis, (1969).

5. L.S. Levine, Experimental Investigation of Normal Ionizing Shock Waves, Phys. Fluids, 11, 1479 (1968).

6. J.B. Heywood, Experiments in a Magnetically Driven Shock Tube with an Axial Magnetic Field, Phys. Fluids, 9, 1150 (1966).

7. R.T. Taussig, Normal Ionizing Shock Waves, Phys. Fluids, 8, 1616 (1965).

8. B. Miller, Experimental Study of Normal Ionizing Shock Waves, Phys. Fluids, 10, 9 (1967).

9. W.B. Kunkel and P.A. Gross, in Plasma Hydromagnetics, D. Bershader, Ed., Stanford University Press, Stanford, California (1962).

10. K. Hain and A.C. Kolb, Fast Theta-Pinch, Nuclear Fusion Supplement, 2, 561, (1962).

11. J. Taylor, Detonations in Condensed Explosives, Clarendon Press, Oxford (1962).

12. J.P. Appleton, Electrical Precursors of Ionizing Shock Waves, Phys. Fluids, 9, 336 (1966).

13. M.J. Lubin and E.L. Resler, Precursor Studies in an Electromagnetically Driven Shock Tube, Phys. Fluids, 10, 1 (1967).

14. D.L. Chubb, Structure of Ionizing Shocks in a Monatomic Gas, Phys. Fluids, 11, 2363 (1968).

15. R.A. Gross, Strong Ionizing Shock Waves, Rev. Mod. Phys., 37, 724 (1965).

16. D. Robinson and P.D. Lenn, Plasma Diagnostics by Spectroscopic Methods, Applied Optics, Vol. 6 (1967).

17. H.R. Griem, Plasma Spectroscopy, McGraw Hill, New York (1964).

18. T.A. McLaughlin, Inductive Magnetic Probe Diagnostics in a Plasma, Naval Postgraduate School Thesis, (1970).

INITIAL DISTRIBUTION LIST

		No. Copies
1.	Defense Documentation Center Cameron Station Alexandria, Virginia 22314	2
2.	Library, Code 0212 Naval Postgraduate School Monterey, California 93940	2
3.	Assoc. Prof. A.W. Cooper, Code 61Cr Department of Physics Naval Postgraduate School Monterey, California 93940	4
4.	Ens. Raymond J. Hogan 8625 Caribbean Blvd. Miami, Florida 33157	1

DOCUMENT CONTROL DATA - R & D

(Security classification of title, body of abstract and indexing annotation must be entered when the overall report is classified)

1. ORIGINATING ACTIVITY (Corporate author)
Naval Postgraduate School
Monterey, California 93940

2a. REPORT SECURITY CLASSIFICATION
Unclassified

2b. GROUP

3. REPORT TITLE
Investigation of Normal Ionizing Shock Waves in Argon

4. DESCRIPTIVE NOTES (Type of report and inclusive dates)
Master's Thesis; June 1972

5. AUTHOR(S) (First name, middle initial, last name)
Raymond Joseph Hogan

6. REPORT DATE	7a. TOTAL NO. OF PAGES	7b. NO. OF REFS
June 1972	63	18

8a. CONTRACT OR GRANT NO.	9a. ORIGINATOR'S REPORT NUMBER(S)
b. PROJECT NO.	
c.	9b. OTHER REPORT NO(S) (Any other numbers that may be assigned this report)
d.	

10. DISTRIBUTION STATEMENT
Approved for public release; distribution unlimited.

11. SUPPLEMENTARY NOTES	12. SPONSORING MILITARY ACTIVITY
	Naval Postgraduate School Monterey, California 93940

13. ABSTRACT

Normal ionizing shock waves in neutral argon gas were generated using a cylindrical theta pinch. Axial propagation of these shock waves has been investigated using photoelectric detectors. Magnetic and electrostatic probes were used to give additional information regarding shock structure. The investigation was carried out using steady state magnetic fields normal to the shock front, with a maximum field of 7200 gauss. Initial gas pressures ranged from 0.02 to 1.0 Torr. The investigations included studies of the effects of initial pressure, magnetic field, and capacitor bank voltage upon the shock velocity. Included is a brief discussion of the theta pinch along with the current theory of normal ionizing shock waves.

KEY WORDS	LINK A		LINK B		LINK C	
	ROLE	WT	ROLE	WT	ROLE	WT
Ionizing Shock Waves						
Theta-pinch						
Shock Structure						
Normal Shocks						

Thesis
H676
c.1
Hogan
136236
Investigation of normal ionizing shock waves in Argon.